Mon. Not. R. Astron. Soc. **396,** 2124–2132 (2009) doi:10.1111/j.1365-2966.2009.14761.x

Experimental and theoretical radiative decay rates for highly excited ruthenium atomic levels and the solar abundance of ruthenium

V. Fivet,[1] P. Quinet,[1,2] P. Palmeri,[1] É. Biémont,[1,2⋆] M. Asplund,[3] N. Grevesse,[4] A. J. Sauval,[5] L. Engström,[6] H. Lundberg,[6] H. Hartman[7] and H. Nilsson[7]

[1]*Astrophysique et Spectroscopie, Université de Mons-Hainaut, B-7000 Mons, Belgium*
[2]*IPNAS, Université de Liège, B15 Sart Tilman, B-4000 Liège, Belgium*
[3]*Max Planck Institute for Astrophysics, Postfach 1317, D-85741 Garching, Germany*
[4]*Centre Spatial de Liège, Avenue Pré Aily, B-4031 Angleur-Liège and Institut d'Astrophysique et de Géophysique, Université de Liège, Allée du 6 Août, 17, B5C, B-4000 Liège, Belgium*
[5]*Observatoire Royal de Belgique, Avenue Circulaire, 3, B-1180 Bruxelles, Belgium*
[6]*Department of Physics, Lund University, PO Box 118, SE-221 00 Lund, Sweden*
[7]*Lund Observatory, Lund University, PO Box 43, SE-221 00 Lund, Sweden*

Accepted 2009 March 9. Received 2009 February 19

ABSTRACT

The solar photospheric abundance of ruthenium is revised on the basis of a new set of oscillator strengths derived for Ru I transitions with wavelengths in the spectral range 2250–4710 Å. The new abundance value (in the usual logarithmic scale where the solar hydrogen abundance is equal to 12.00), $A_{\rm Ru} = 1.72 \pm 0.10$, is in agreement with the most recent meteoritic result, $A_{\rm Ru} = 1.76 \pm 0.03$. The accuracy of the transition probabilities, obtained using a relativistic Hartree–Fock model including core-polarization effects, has been assessed by comparing the theoretical lifetimes with previous experimental results. A comparison is also made with new measurements performed in this work by the time-resolved laser-induced fluorescence spectroscopy for 10 highly excited odd-parity levels of Ru I.

Key words: atomic data – atomic processes – Sun: abundances.

1 INTRODUCTION

Ruthenium is a transition metal ($Z = 44$) of the palladium group having seven stable isotopes ($A = 96, 98, 99, 100, 101, 102$ and 104) occurring with the natural abundances 5.5, 1.9, 12.8, 12.6, 17.1, 31.6 and 18.6 per cent, respectively (Asplund et al. 2009). There exist also several short-lived radioisotopes used in different scientific and medical applications, such as nuclear magnetic resonance, material physics and microelectronics.

In stars, ruthenium isotopes are generated by different nucleosynthesis processes. ^{96}Ru and ^{98}Ru are pure *p*-products, ^{100}Ru is produced by the *s*-process and ^{104}Ru by the *r*-process. ^{99}Ru, ^{101}Ru and ^{102}Ru can be generated by both the *r*- and *s*-processes. ^{100}Ru is particularly interesting because it is produced during *s*-process reactions when a neutron is captured by a ^{99}Tc atom.

Ruthenium plays an important role in stellar nucleosynthesis. When the stars are in the 'asymptotic giant branch (AGB)' phase, they experience thermal pulses, generating a rich nucleosynthesis by the *s*-process. The convective envelope of the star may penetrate the region where *s*-process elements have been produced, and may bring them to the stellar surface, where they become observable. A few *s*-process elements are particularly interesting in that respect because they provide information on the time-scales involved in the process. Ruthenium is among these elements.

The ruthenium abundance, and also that of other elements such as Nb or Tc, is thus very important in order to constrain evolutionary lifetimes during the thermally pulsing AGB phase. However, relatively few investigations have been devoted to the time evolution of these heavy elements in stars due to the difficulty in deriving accurate abundances in the crowded spectra of the stars in their AGB phase.

In the past, neutral ruthenium has been detected in different types of stars. More specifically, Ru I has been observed in at least one Ap star of the Cr–Eu–Sr subgroup (Jaschek & Brandi 1972) and this element was shown to be enhanced in S-type stars (Smith & Wallerstein 1983) and in subgiant CH stars (Krishnaswamy & Sneden 1985), leading to an overabundance reaching one order of magnitude. An analysis of the ruthenium abundance in the atmospheres of three K giant stars was also reported by Orlov & Shavrina (1990) who used two Ru I lines. More recently, the abundance of ruthenium was determined through the spectrum synthesis of two lines observed in the spectra of dwarf and giant barium stars (Allen & Porto de Mello 2008).

In the sun, nine Ru I lines, identified in the solar photospheric spectrum at λλ 3436.737, 3742.280, 3755.931, 3798.901, 3799.347,

⋆E-mail: E.biemont@ulg.ac.be

4554.509, 4584.445, 5057.331 and 5309.267 Å, were used to derive the solar content of this element (Biémont et al. 1984) on the basis of the Holweger & Müller (1974) model. This analysis, however, suffered from the lack of accurate branching fractions (BF), the only values available at that time being those of Corliss & Bozman (1962). In addition, this work represented a standard stellar abundance analysis based on a time-independent one-dimensional (1D) model atmosphere in hydrodynamic equilibrium. Since that time, there has been a progress concerning our knowledge of the atmosphere of the sun with the advent of new three-dimensional (3D), time-dependent, hydrodynamical models (see e.g. Asplund 2005; Asplund et al. 2009). As a consequence, a new determination of the solar abundance of ruthenium is now needed.

For stellar (and solar) abundance determinations, the transition probabilities remain the key input data. In Ru I, they are still poorly known despite some attempts made in the past to improve *gf* values (see Section 2). The need for new transition probabilities and the gaps in the existing data have even prompted some authors to deduce astrophysical *f* values (see e.g. Thévenin 1989, 1990).

As a consequence, this paper reports on a calculation of new transition probabilities in neutral ruthenium using a relativistic Hartree–Fock (HFR) model including core-polarization (CPOL) contributions. The adequacy of the theoretical approach has been tested by a comparison of the derived theoretical lifetimes with the experimental results published by Salih & Lawler (1985) for energies up to 38 200 cm^{-1} and with new accurate laser measurements obtained, in this work, for some higher energy levels (up to 47 248 cm^{-1}).

2 PREVIOUS WORK

The ground state of Ru I is $4d^7(^4F)5s\ ^5F_5$ and the first excited configurations are $4d^65s^2$, $4d^8$, $4d^65s5p$ and $4d^75p$. The critical compilation of energy levels in this atom by Moore (1971) is based on previous analyses by Kessler & Meggers (1955) and Kessler (unpubl. data). An extensive theoretical study by Trees (unpubl. data) confirmed the observed values for the low even terms and allowed to make a number of the spectroscopic assignments for additional terms. At present, 100 even and 205 odd levels are known, and there are approximately 3250 classified lines between 2013.95 and 11 483.91 Å. In this work (see Section 4), we adopted the energy levels of Ru I taken from the compilation of Moore (1971).

The first experimental determination of oscillator strengths in Ru I is due to Corliss & Bozman (1962) who performed arc measurements for 909 transitions in the spectral range 2076–8777 Å. Unfortunately, it is now well established that these results are affected by large systematic errors.

About 25 years ago, radiative lifetimes were measured by laser excitation for 12 levels ranging from 26 313 to 39 434 cm^{-1} and belonging to the $4d^75p$ and $4d^65s5p$ configurations of neutral ruthenium (Biémont et al. 1984). More recently, experimental absolute transition probabilities for 482 Ru I lines, involving odd-parity levels up to 38 200 cm^{-1}, were published by Wickliffe, Salih & Lawler (1994). These *A* values were determined from a combination of BFs, measured using the Fourier transform spectrometer of the National Solar Observatory on Kitt Peak, with radiative lifetimes previously obtained using time-resolved laser-induced fluorescence (TR-LIF) spectroscopy on a slow Ru atomic beam (Salih & Lawler 1985).

The main purpose of this work is to provide a homogeneous set of *f* values for all the astrophysically important transitions of Ru I and to extend the data available to transitions for which oscillator strengths are still missing, particularly for transitions involving highly excited states.

3 TR-LIF LIFETIME MEASUREMENTS

In this work, we report on lifetime measurements of 10 short-lived odd-parity levels of Ru I obtained with the TR-LIF spectroscopy on a laser-produced plasma. This technique is well adapted for providing accurate lifetime values in many neutral, singly ionized or doubly ionized heavy ions (see e.g. Biémont & Quinet 2003; Biémont 2005).

The experimental setup used in the present experiment has been described elsewhere (see e.g. Xu et al. 2003, 2004; Fivet et al. 2006; Nilsson et al. 2008) and only a brief description will be provided here.

The ruthenium atoms were generated in a laser-produced plasma by focusing a 532 nm Nd:YAG laser (Continuum Surelite) pulse on to a rotating ruthenium target. With this device, free ruthenium atoms can be produced in the ground as well as in metastable states from where the studied levels can be excited. In addition, the plasma density and temperature can be controlled and adjusted by changing the pulse energy and the beam size on the target. Another advantage of the experimental setup is that neutral and ionized atoms, produced in the plasma, have different velocities and therefore can be separated by selecting appropriate delay times between the ablation and the excitation pulses (see e.g. Xu et al. 2004).

The excitation pulses have a duration of about 1 ns. This is achieved by sending a frequency-doubled Nd:YAG laser (Continuum NY-82) pulse into a temporal compressor, based on stimulated Brillouin scattering (SBS) in water. The Nd:YAG laser consists of an injection seeding system which results in a single longitudinal mode pulsed output and improves significantly the laser energy stability. In order to generate the required excitation wavelengths, the compressed pulses were used to pump a dye laser (Continuum Nd-60). Using the DCM (4-dicyanomethylene-2-methyl-6-p-dimethylaminostyryl-4H-pyran) dye, the region of the required excitation wavelengths can be covered by different non-linear processes, such as frequency upconversion in KDP (potassium dihydrogen phosphate) and BBO (β-baryum borate) crystals and the stimulated Raman scattering in a hydrogen gas cell (10 bar).

The excitation beam interacted with the neutral ruthenium atoms about 1 cm above the foil target. The fluorescence, emitted from the excited levels, was collected by a fused silica lens and focused on to the entrance slit of a 1/8 m monochromator, and then detected by a Hamamatsu 1564U microchannel plate photomultiplier tube, which had a risetime of 0.2 ns.

The experimental values of the 10 measured lifetimes are reported in Table 1. The uncertainties of the values in the table take into account statistical errors as well as the reproducibility of the results between repeated measurements. Table 1 also includes the experimental results obtained previously (Biémont et al. 1984; Salih & Lawler 1995) and the theoretical values obtained in this work.

4 RELATIVISTIC HARTREE–FOCK CALCULATIONS

The theoretical method used in this paper is the HFR approach (Cowan 1981) in which we have incorporated the CPOL and core-penetration effects. Intravalence-type interactions have been considered by including, in the configuration interaction expansions, the configurations $4d^75s$, $4d^76s$, $4d^75d$, $4d^76d$, $4d^8$, $4d^65s^2$, $4d^65p^2$,

Table 1. Experimental and calculated lifetimes (τ, in ns) for Ru I odd-parity levels.

E (cm^{-1})[a]	Configuration[a]	Level[a]	τ (experiment)			τ (theory)
			BGKZ[b]	SL[c]	This work	This work
25 214.16	4d^{6}5s5p	z ^{7}D$^\circ_5$		2100 ± 210		*
25 464.49	4d^{6}5s5p	z ^{7}D$^\circ_4$		141 ± 7		*
26 035.56	4d^{6}5s5p	z ^{7}D$^\circ_3$		901 ± 45		*
26 312.83	4d^{7}5p	z ^{5}D$^\circ_4$	17.3 ± 0.9	16.3 ± 0.8		15.5
26 816.23	4d^{7}5p	z ^{5}F$^\circ_5$	11.2 ± 0.6	11.6 ± 0.6		10.9
27 506.59	4d^{7}5p	z ^{5}D$^\circ_3$	15.2 ± 0.8	14.5 ± 0.7		12.9
28 014.79	4d^{7}5p	z ^{5}F$^\circ_4$		12.0 ± 0.6		11.0
28 465.69	4d^{7}5p	z ^{5}D$^\circ_2$		14.3 ± 0.7		12.7
28 495.10	4d^{7}5p	z ^{3}G$^\circ_5$	12.2 ± 0.6	12.6 ± 0.6		12.1
28 571.89	4d^{7}5p	z ^{5}G$^\circ_6$		11.6 ± 0.6		15.1
28 890.47	4d^{7}5p	z ^{5}F$^\circ_3$		12.2 ± 0.6		11.2
29 118.49	4d^{7}5p	z ^{5}D$^\circ_1$		14.2 ± 0.7		12.7
29 427.32	4d^{7}5p	z ^{5}F$^\circ_2$	12.5 ± 0.6	12.8 ± 0.6		11.6
29 468.04	4d^{6}5s5p	z ^{7}F$^\circ_5$		134 ± 7		*
29 569.90	4d^{7}5p	z ^{5}D$^\circ_0$		16.0 ± 0.8		14.2
29 594.56	4d^{6}5s5p	z ^{7}F$^\circ_4$		29.3 ± 1.5		*
29 693.57	4d^{7}5p	z ^{5}F$^\circ_1$		13.1 ± 0.6		11.8
29 890.91	4d^{7}5p	z ^{3}G$^\circ_4$	16.2 ± 0.8	17.7 ± 0.9		11.5
29 891.90	4d^{6}5s5p	z ^{7}F$^\circ_3$		243 ± 12		*
30 085.38	4d^{6}5s5p	z ^{7}F$^\circ_1$		663 ± 66		*
30 250.40	4d^{6}5s5p	z ^{7}P$^\circ_4$		99 ± 5		*
30 279.68	4d^{7}5p	z ^{5}G$^\circ_5$	9.4 ± 0.5	9.8 ± 0.5		8.9
30 348.45	4d^{7}5p	z ^{3}F$^\circ_4$	11.9 ± 0.6	12.2 ± 0.6	12.8 ± 0.9	13.6
30 537.06	4d^{7}5p	z ^{5}G$^\circ_3$	10.2 ± 0.5	10.0 ± 0.5		9.4
30 958.80	4d^{7}5p	z ^{5}G$^\circ_2$	10.3 ± 0.5	9.2 ± 0.5		8.8
31 044.35	4d^{7}5p	z ^{3}D$^\circ_3$		10.9 ± 0.5		10.9
31 186.03	4d^{7}5p	z ^{5}S$^\circ_2$		21.8 ± 1.1		22.7
31 345.79	4d^{7}5p	z ^{5}G$^\circ_4$		11.1 ± 0.5		10.4
31 852.90	4d^{7}5p	z ^{3}G$^\circ_3$		11.9 ± 0.6		11.6
32 207.65	4d^{7}5p	z ^{3}D$^\circ_2$		12.8 ± 0.6		19.0
32 391.95	4d^{7}5p	z ^{3}F$^\circ_3$		10.4 ± 0.5		10.4
33 172.02	4d^{7}5p	z ^{3}F$^\circ_2$		10.1 ± 0.5		10.2
33 430.65	4d^{6}5s5p	y ^{5}D$^\circ_3$		19.3 ± 1.0		17.8
33 446.84	4d^{6}5s5p	y ^{5}D$^\circ_4$	14.6 ± 0.7	14.9 ± 0.7		14.6
33 580.22	4d^{7}5p	z ^{3}D$^\circ_1$		10.4 ± 0.5		10.6
33 728.66	4d^{6}5s5p	y ^{5}D$^\circ_2$		19.3 ± 1.0		17.6
34 072.41	4d^{6}5s5p	z ^{5}P$^\circ_3$		24.9 ± 1.2		20.3
34 091.06	4d^{6}5s5p	y ^{5}D$^\circ_1$		18.8 ± 0.9		17.0
34 772.55	4d^{6}5s5p	y ^{5}F$^\circ_5$		14.0 ± 0.7		13.5
34 881.92	4d^{6}5s5p	z ^{5}P$^\circ_2$		23.3 ± 1.2		18.7
35 046.77	4d^{6}5s5p	z ^{5}P$^\circ_1$		22.9 ± 1.1		18.5
35 471.15	4d^{6}5s5p	y ^{5}F$^\circ_4$		15.5 ± 0.8		14.8
35 806.62	4d^{6}5s5p	y ^{5}F$^\circ_3$		15.4 ± 0.8		14.8
35 963.87	4d^{6}5s5p	y ^{5}F$^\circ_2$		16.8 ± 0.8		15.4
36 760.34	4d^{7}5p	y ^{3}D$^\circ_3$		7.8 ± 0.4		7.9
36 965.28	4d^{7}5p	y ^{3}D$^\circ_2$		13.8 ± 0.7		12.0
37 118.90	4d^{7}5p	z ^{3}P$^\circ_2$		9.5 ± 0.5		10.0
37 367.02	4d^{7}5p	x ^{5}D$^\circ_3$		9.7 ± 0.5		9.6
37 667.86	4d^{7}5p	x ^{5}D$^\circ_2$		10.1 ± 0.5		10.2
38 200.40	4d^{7}5p	x ^{5}D$^\circ_1$		8.1 ± 0.4	8.6 ± 0.8	9.0
39 433.70	4d^{7}5p	y ^{3}F$^\circ_3$	10.3 ± 0.5			9.1
39 742.03	4d^{7}5p	y ^{3}P$^\circ_2$			10.8 ± 1.0	9.6
40 768.15	4d^{7}5p	x ^{3}D$^\circ_3$			9.7 ± 0.9	8.6
41 182.94	4d^{7}5p	x ^{3}F$^\circ_2$			8.5 ± 0.9	8.6
41 260.04	4d^{7}5p	x ^{3}F$^\circ_3$			9.5 ± 0.9	8.5
42 346.90	4d^{7}5p	x ^{3}F$^\circ_4$			12.0 ± 1.2	10.8
44 321.81	4d^{6}5s5p	x ^{5}F$^\circ_5$			10.0 ± 0.9	10.4

Table 1 – *continued*

E (cm^{-1})[a]	Configuration[a]	Level[a]	τ (experiment) BGKZ[b]	SL[c]	This work	τ (theory) This work
44 607.61	$4d^6 5s5p$	x $^5F^\circ_4$			8.9 ± 0.9	8.6
47 247.98	$4d^7 6p$	w $^3F^\circ_2$			13.5 ± 1.0	*

[a]Moore (1971).
[b]Biémont et al. (1984).
[c]Salih & Lawler (1985).
*See the text.

$4d^6 5d^2$, $4d^6 5s6s$, $4d^6 5s5d$, $4d^6 5s6d$ (even parity) and $4d^7 5p$, $4d^7 6p$, $4d^7 4f$, $4d^7 5f$, $4d^6 5s5p$, $4d^6 5s6p$, $4d^6 5p5d$, $4d^6 5p6s$ (odd parity). Core-valence interactions were taken into account using a CPOL potential and a correction to the dipole operator following a well-established procedure giving rise to the HFR+CPOL method (see e.g. Quinet et al. 1999; Biémont & Quinet 2003). For the dipole polarizability, α_d, we used the value computed by Fraga, Karwowski & Saxena (1976) for the ionic core Ru III, i.e. $\alpha_d = 8.03 a_0^3$. The value of the cut-off radius, r_c, was the HFR mean value $\langle r \rangle$ of the outermost 4d core orbital, i.e. $r_c = 1.60 a_0$.

Some radial integrals, considered as free parameters, were then adjusted with a least-squares optimization program minimizing the discrepancies between the calculated Hamiltonian eigenvalues and the experimental energy levels taken from Moore (1971). More precisely, for the $4d^7 5s$, $4d^8$ and $4d^6 5s^2$ even configurations, the average energies (E_{av}), the electrostatic direct (F^k) and exchange (G^k) integrals, the spin-orbit integrals (ζ_{nl}) and the effective parameters (α) were allowed to vary during the fitting process. An additional effective operator (β) for the $4d^7 5s$ configuration was also included in this adjustment. The dubious experimental $4d^8\,^3P_0$ level at 24 173.68 cm^{-1} (appearing with a question mark in the Moore's compilation) was not included in the fit because the discrepancy with the corresponding *ab initio* computed energy was larger than the mean difference observed for all the other even levels indicating a wrong assignment in Moore's (1971) table. For the odd parity, only the experimental levels below 45 000 cm^{-1} were used to optimize all the E_{av}, F^k, G^k, ζ_{nl} and α parameters belonging to the $4d^7 5p$ and $4d^6 5s5p$ configurations. The configuration interaction integrals (R^k) between these two configurations were also adjusted with the constraint that the ratio between them was not allowed to vary. Above 45 000 cm^{-1}, due to the large number of calculated odd-parity levels and the strong mixing between these states, it was extremely difficult to establish an unambiguous correspondence between the calculated and the few experimental values. Even the use of available Landé g factors (see Section 7) did not help in making the identifications more reliable. The average deviations of the fits were 84 cm^{-1} for the even parity and 189 cm^{-1} for the odd parity.

5 RESULTS AND DISCUSSION

A comparison of the calculated lifetimes with the measurements performed by Biémont et al. (1984) and Salih & Lawler (1985) and in this work is reported in Table 1. As seen from this table, the agreement between theory and experiment is very good, the average of the ratio τ_{exp}/τ_{th} being 1.06 ± 0.12. However, it is important to note that, for the eight levels situated at 25 214.16, 25 464.49, 26 035.56, 29 468.04, 29 594.56, 29 891.90, 30 085.38 and 30 250.40 cm^{-1}, no theoretical lifetimes are given in the table although experimental values were published by Salih & Lawler (1985). The reason is that, for all these levels, belonging to the z $^7P^\circ$, z $^7D^\circ$ and z $^7F^\circ$ multiplets of the $4d^6 5s5p$ configuration, the computed lifetimes are very sensitive to small changes in the eigenvector compositions. As an example, when varying the main components of the $4d^6 5s5p$ z$^7P^\circ$, z$^7D^\circ$ and z$^7F^\circ$ levels by less than a per cent, the corresponding lifetimes changed by 10–30 per cent. Moreover, some of the calculated line strengths for transitions depopulating these septet levels, able to decay only by intercombination lines, were found to be affected by severe cancellation effects.

For the two levels at 30 348.45 and 38 200.40 cm^{-1}, our new measurements agree (within the experimental uncertainties) with the previous LIF measurements of Biémont et al. (1984) and of Salih & Lawler (1995), whereas for the eight excited levels there are no previous values to compare with.

Table 2 shows the weighted transition probabilities (gA, g being the statistical weight of the upper level of the transition) and oscillator strengths (log gf, g being the statistical weight of the lower level of the transition), as calculated in this work, for selected transitions in Ru I. Due to space limitations, only transitions with gA values larger than 10^8 s^{-1} are reported in the table. Our results are also compared with the experimental values previously published by Wickliffe et al. (1994). The results for the weaker transitions are available from the authors.

In Fig. 1, we show a more detailed comparison between our log gf values (HFR+CPOL) and those reported by Wickliffe et al. (1994) (EXP). The straight line in the figure corresponds to the equality of the two sets of data. Our results appear in good agreement (within 10–20 per cent in general) with those obtained experimentally for the strongest lines, i.e. for transitions with $\log gf > -1$. For weaker transitions, a somewhat larger scatter is observed when comparing theoretical and experimental values. On the theoretical side, this is due to level mixing and cancellation effects. On the experimental side, smaller BFs have larger uncertainties.

6 THE SOLAR ABUNDANCE OF RUTHENIUM

The most recent analysis of ruthenium lines in the solar photospheric spectrum was in fact made 25 years ago by Biémont et al. (1984) who used a sample of nine faint solar Ru I lines together with the Holweger & Müller (1974) model and gf values measured in the same work (see Section 2) to derive an abundance of ruthenium, $A_{Ru} = 1.84 \pm 0.10$.

We predicted the equivalent widths of the strongest of the Ru I and Ru II lines for which new accurate gf values have been obtained in this work. These lines have then been searched for and carefully examined and measured on two solar spectra recorded at the centre of the solar disc by Delbouille, Neven & Roland (1973) and Neckel & Labs (1984). We finally retained the six Ru I lines, given in Table 3, as good indicators of the abundance of ruthenium. All the other lines are either heavily blended or impossible to treat

Table 2. Transition probabilities (gA) and oscillator strengths ($\log gf$) for Ru I transitions. Only transitions with $E < 45\,000\,\mathrm{cm}^{-1}$ and $gA > 10^8\,\mathrm{s}^{-1}$ are listed in the table. $A(B)$ stands for $A \times 10^B$.

λ (Å)[a]	Lower level		Upper level		Theory		Experiment	
	E (cm^{-1})[b]	Desig.[b]	E (cm^{-1})[b]	Desig.[b]	gA (s^{-1})[c]	$\log gf$[c]	gA (s^{-1})[d]	$\log gf$[d]
2255.527	0.00	a ^{5}F$_5$	44 321.81	x ^{5}F$^\circ_5$	3.64(8)	−0.56		
2272.097	0.00	a ^{5}F$_5$	43 998.60	2°(^{5}G°)$_6$	1.61(8)	−0.90		
2317.797	1190.64	a ^{5}F$_4$	44 321.81	x ^{5}F$^\circ_5$	6.79(8)	−0.27		
2328.164	0.00	a ^{5}F$_5$	42 939.12	x ^{3}G$^\circ_4$	6.02(8)	0.13		
2336.543	1190.64	a ^{5}F$_4$	43 975.79	x ^{3}G$^\circ_3$	3.61(8)	−0.52		
2372.141	2091.54	a ^{5}F$_3$	44 234.68	x ^{3}P$^\circ_2$	1.85(8)	−0.81		
2386.805	2091.54	a ^{5}F$_3$	43 975.79	x ^{3}G$^\circ_3$	1.68(8)	−0.84		
2394.567	1190.64	a ^{5}F$_4$	42 939.12	x ^{3}G$^\circ_4$	1.48(8)	−0.90		
2407.662	2713.24	a ^{5}F$_2$	44 234.68	x ^{3}P$^\circ_2$	1.24(8)	−0.97		
2687.534	6545.03	a ^{3}F$_4$	43 742.81	w ^{3}G$^\circ_5$	3.52(8)	−0.42		
2688.896	7483.07	a ^{5}D$_4$	44 662.01	y ^{3}H$^\circ_4$	1.91(8)	−0.68		
2729.467	7483.07	a ^{5}D$_4$	44 109.41	y ^{3}H$^\circ_5$	6.02(8)	−0.17		
2733.083	8084.12	a ^{3}F$_3$	44 662.01	y ^{3}H$^\circ_4$	4.99(8)	−0.25		
2735.721	0.00	a ^{5}F$_5$	36 542.62	x ^{5}D$^\circ_4$	7.52(8)	−0.07		
2739.462	7483.07	a ^{5}D$_4$	43 975.79	x ^{3}G$^\circ_3$	6.82(8)	−0.11		
2746.886	6545.03	a ^{3}F$_4$	42 939.12	x ^{3}G$^\circ_4$	3.48(8)	−0.40		
2752.795	8575.42	a ^{5}D$_3$	44 891.40	5°(^{5}G°)$_2$	2.32(8)	−0.57		
2757.065	7483.07	a ^{5}D$_4$	43 742.81	w ^{3}G$^\circ_5$	2.46(9)	0.45		
2765.392	8084.12	a ^{3}F$_3$	44 234.68	x ^{3}P$^\circ_2$	1.00(8)	−0.94		
2768.229	7483.07	a ^{5}D$_4$	43 596.58	y ^{1}H$^\circ_5$	2.28(8)	−0.59		
2770.294	8575.42	a ^{5}D$_3$	44 662.01	y ^{3}H$^\circ_4$	1.97(9)	0.36		
2782.206	8043.69	a ^{5}P$_2$	43 975.79	x ^{3}G$^\circ_3$	1.41(8)	−0.78		
2785.340	8084.12	a ^{3}F$_3$	43 975.79	x ^{3}G$^\circ_3$	2.77(8)	−0.49		
2789.842	9057.64	a ^{5}D$_2$	44 891.40	5°(^{5}G°)$_2$	1.74(8)	−0.69		
2803.494	8575.42	a ^{5}D$_3$	44 234.68	x ^{3}P$^\circ_2$	4.05(8)	−0.32		
2810.554	1190.64	a ^{5}F$_4$	36 760.34	y ^{3}D$^\circ_3$	4.76(8)	−0.25	4.68(8)	−0.26
2819.563	7483.07	a ^{5}D$_4$	42 939.12	x ^{3}G$^\circ_4$	2.05(9)	0.39		
2822.030	8084.12	a ^{3}F$_3$	43 509.17	u ^{3}D$^\circ_2$	1.16(8)	−0.87		
2823.998	8575.42	a ^{5}D$_3$	43 975.79	x ^{3}G$^\circ_3$	7.04(8)	−0.07		
2829.157	6545.03	a ^{3}F$_4$	41 880.85	v ^{3}D$^\circ_3$	3.86(8)	−0.34		
2836.568	9057.64	a ^{5}D$_2$	44 301.14	3°(^{3}P°)$_1$	1.22(8)	−0.83		
2840.536	6545.03	a ^{3}F$_4$	41 739.30	x ^{3}G$^\circ_5$	1.06(8)	−0.89		
2841.928	9057.64	a ^{5}D$_2$	44 234.68	x ^{3}P$^\circ_2$	1.62(8)	−0.71		
2843.168	9072.98	a ^{5}D$_1$	44 234.68	x ^{3}P$^\circ_2$	2.17(8)	−0.58		
2852.146	9183.66	a ^{3}F$_2$	44 234.68	x ^{3}P$^\circ_2$	1.01(8)	−0.91		
2866.645	2091.54	a ^{5}F$_3$	36 965.28	y ^{3}D$^\circ_2$	2.04(8)	−0.60	1.20(8)	−0.83
2868.307	8043.69	a ^{5}P$_2$	42 897.23	v ^{3}D$^\circ_2$	1.15(8)	−0.84		
2874.988	0.00	a ^{5}F$_5$	34 772.55	y ^{5}F$^\circ_5$	4.92(8)	−0.22	4.63(8)	−0.24
2879.753	6545.03	a ^{3}F$_4$	41 260.04	x ^{3}F$^\circ_3$	1.02(8)	−0.90		
2886.531	2713.24	a ^{5}F$_2$	37 346.74	z ^{3}P$^\circ_1$	2.01(8)	−0.60		
2909.195	8575.42	a ^{5}D$_3$	42 939.12	x ^{3}G$^\circ_4$	1.44(8)	−0.74		
2916.256	1190.64	a ^{5}F$_4$	35 471.15	y ^{5}F$^\circ_4$	2.59(8)	−0.48	2.20(8)	−0.55
2921.146	6545.03	a ^{3}F$_4$	40 768.15	x ^{3}D$^\circ_3$	3.22(8)	−0.38		
2925.842	8770.93	a ^{5}P$_3$	42 939.12	x ^{3}G$^\circ_4$	1.61(8)	−0.68		
2949.493	6545.03	a ^{3}F$_4$	40 439.25	1°(^{3}F°)$_4$	1.97(8)	−0.59		
2965.166	2091.54	a ^{5}F$_3$	35 806.62	y ^{5}F$^\circ_3$	1.95(8)	−0.59	1.72(8)	−0.64
2968.957	8084.12	a ^{3}F$_3$	41 756.15	z ^{1}D$^\circ_2$	1.27(8)	−0.77		
2988.947	0.00	a ^{5}F$_5$	33 446.84	y ^{5}D$^\circ_4$	2.57(8)	−0.46	2.25(8)	−0.52
2993.270	8084.12	a ^{3}F$_3$	41 482.66	w ^{3}D$^\circ_3$	1.42(8)	−0.73		
2994.967	2091.54	a ^{5}F$_3$	35 471.15	y ^{5}F$^\circ_4$	1.02(8)	−0.86	9.90(7)	−0.88
3006.585	2713.24	a ^{5}F$_2$	35 963.87	y ^{5}F$^\circ_2$	1.38(8)	−0.73	1.15(8)	−0.81
3010.419	10 654.62	b ^{3}F$_3$	43 862.91	w ^{3}G$^\circ_4$	4.95(8)	−0.15		
3017.235	3105.49	a ^{5}F$_1$	36 238.77	y ^{5}F$^\circ_1$	1.08(8)	−0.83		
3019.780	11 786.05	a ^{3}P$_1$	44 891.40	5°(^{5}G°)$_2$	1.39(8)	−0.72		
3020.376	8084.12	a ^{3}F$_3$	41 182.94	x ^{3}F$^\circ_2$	1.27(8)	-0.76		
3042.833	10 654.62	b ^{3}F$_3$	43 509.17	u ^{3}D$^\circ_2$	1.06(8)	−0.84		
3064.838	9120.63	b ^{3}F$_4$	41 739.30	x ^{3}G$^\circ_5$	6.09(8)	−0.07		
3089.144	9120.63	b ^{3}F$_4$	41 482.66	w ^{3}D$^\circ_3$	1.12(8)	−0.80		
3097.599	10 623.53	a ^{3}P$_2$	42 897.23	v ^{3}D$^\circ_2$	1.64(8)	−0.63		
3168.555	11 447.31	b ^{3}F$_2$	42 998.31	y ^{1}F$^\circ_3$	1.27(8)	−0.72		
3188.372	11 752.62	a ^{3}P$_0$	43 107.52	y ^{3}S$^\circ_1$	1.53(8)	−0.63		

Table 2 – *continued*

λ (Å)[a]	Lower level		Upper level		Theory		Experiment	
	E (cm^{-1})[b]	Desig.[b]	E (cm^{-1})[b]	Desig.[b]	gA (s^{-1})[c]	log gf[c]	gA (s^{-1})[d]	log gf[d]
3199.521	13 645.75	b ^{3}P$_2$	44 891.40	5°(^{5}G°)$_2$	2.11(8)	−0.48		
3228.528	8043.69	a ^{5}P$_2$	39 008.62	y ^{5}P°$_2$	1.15(8)	−0.75		
3260.354	8043.69	a ^{5}P$_2$	38 706.36	y ^{5}P°$_3$	1.52(8)	−0.62		
3268.214	13 645.75	b ^{3}P$_2$	44 234.68	x ^{3}P°$_2$	1.31(8)	−0.68		
3296.647	10 623.53	a ^{3}P$_2$	40 948.65	z ^{1}F°$_3$	2.12(8)	−0.46		
3306.179	8770.93	a ^{5}P$_3$	39 008.62	y ^{5}P°$_2$	1.14(8)	−0.74		
3339.563	8770.93	a ^{5}P$_3$	38 706.36	y ^{5}P°$_3$	6.54(8)	0.03		
3341.671	9120.63	b ^{3}F$_4$	39 037.18	z ^{1}G°$_4$	1.79(8)	−0.53		
3401.735	9620.29	a ^{5}P$_1$	39 008.62	y ^{5}P°$_2$	1.56(8)	−0.58		
3409.276	8043.69	a ^{5}P$_2$	37 367.02	x ^{5}D°$_3$	1.29(8)	−0.64	1.38(8)	−0.62
3417.327	2091.54	a ^{5}F$_3$	31 345.79	z ^{5}G°$_4$	3.40(8)	−0.23	3.15(8)	−0.26
3429.553	10 623.53	a ^{3}P$_2$	39 773.49	y ^{5}P°$_1$	1.44(8)	−0.61		
3432.757	9120.63	b ^{3}F$_4$	38 243.38	y ^{3}F°$_4$	2.02(8)	−0.45		
3433.259	10 623.53	a ^{3}P$_2$	39 742.03	y ^{3}P°$_2$	1.09(8)	−0.72		
3436.736	1190.64	a ^{5}F$_4$	30 279.68	z ^{5}G°$_5$	8.60(8)	0.18	8.01(8)	0.15
3438.370	8043.69	a ^{5}P$_2$	37 118.90	z ^{3}P°$_2$	1.14(8)	−0.69	9.50(7)	−0.77
3448.963	11 447.31	b ^{3}F$_2$	40 433.23	y ^{3}F°$_2$	1.07(8)	−0.72		
3473.752	10 654.62	b ^{3}F$_3$	39 433.70	y ^{3}F°$_3$	1.60(8)	−0.54		
3498.942	0.00	a ^{5}F$_5$	28 571.89	z ^{5}G°$_6$	8.62(8)	0.20	1.12(9)	0.31
3532.810	14 700.32	a ^{1}G$_4$	42 998.31	y ^{1}F°$_3$	2.62(8)	−0.31		
3553.846	11 786.05	a ^{3}P$_1$	39 916.54	y ^{3}P°$_1$	1.49(8)	−0.56		
3587.156	16 240.13	a ^{3}H$_5$	44 109.41	y ^{3}H°$_5$	7.74(8)	0.18		
3589.213	3105.49	a ^{5}F$_1$	30 958.80	z ^{5}G°$_2$	4.77(8)	−0.04	4.56(8)	−0.06
3593.017	2713.24	a ^{5}F$_2$	30 537.06	z ^{5}G°$_3$	6.15(8)	0.08	5.72(8)	0.04
3596.157	12 816.69	a ^{3}G$_4$	40 616.22	z ^{1}H°$_5$	1.18(8)	−0.65		
3596.178	2091.54	a ^{5}F$_3$	29 890.91	z ^{3}G°$_4$	5.96(8)	0.07	3.78(8)	−0.13
3599.762	8770.93	a ^{5}P$_3$	36 542.62	x ^{5}D°$_4$	5.44(8)	0.03		
3601.476	16 240.13	a ^{3}H$_5$	43 998.60	2°(^{5}G°)$_6$	1.01(8)	−0.70		
3619.168	16 240.13	a ^{3}H$_5$	43 862.91	w ^{3}G°$_4$	5.91(8)	0.09		
3625.194	10 623.53	a ^{3}P$_2$	38 200.40	x ^{5}D°$_1$	1.08(8)	−0.67	1.10(8)	−0.67
3633.908	17 096.87	a ^{3}H$_4$	44 607.61	x ^{5}F°$_4$	8.04(8)	0.20		
3634.973	16 240.13	a ^{3}H$_5$	43 742.81	w ^{3}G°$_5$	1.27(8)	−0.60		
3649.179	17 045.97	a ^{1}D$_2$	44 441.59	4°(?°)$_3$	1.15(8)	−0.63		
3655.971	17 096.87	a ^{3}H$_4$	44 441.59	4°(?°)$_3$	2.97(8)	−0.21		
3660.815	16 240.13	a ^{3}H$_5$	43 548.67	y ^{3}H°$_6$	2.76(8)	−0.26		
3661.362	1190.64	a ^{5}F$_4$	28 495.10	z ^{3}G°$_5$	4.80(8)	−0.01	4.57(8)	−0.04
3663.372	7483.07	a ^{5}D$_4$	34 772.55	y ^{5}F°$_5$	2.08(8)	−0.38	1.85(8)	−0.43
3669.540	12 207.05	a ^{3}G$_5$	39 450.66	y ^{3}G°$_5$	4.35(8)	−0.05		
3700.931	17 096.87	a ^{3}H$_4$	44 109.41	y ^{3}H°$_5$	1.43(8)	−0.53		
3717.005	8575.42	a ^{5}D$_3$	35 471.15	y ^{5}F°$_4$	1.08(8)	−0.65	6.80(7)	−0.85
3722.784	15 550.16	a ^{3}H$_6$	42 404.14	z ^{1}I°$_6$	1.30(9)	0.40		
3726.093	12 207.05	a ^{3}G$_5$	39 037.18	z ^{1}G°$_4$	3.20(8)	−0.18		
3726.924	1190.64	a ^{5}F$_4$	28 014.79	z ^{5}F°$_4$	7.48(8)	0.20	6.78(8)	0.15
3728.025	0.00	a ^{5}F$_5$	26 816.23	z ^{5}F°$_5$	9.72(8)	0.31	9.02(8)	0.27
3730.431	2091.54	a ^{5}F$_3$	28 890.47	z ^{5}F°$_3$	5.43(8)	0.06	4.94(8)	0.01
3738.911	16 240.13	a ^{3}H$_5$	42 978.28	z ^{3}I°$_5$	2.03(8)	−0.37		
3739.469	13 699.07	a ^{3}G$_3$	40 433.23	y ^{3}F°$_2$	1.83(8)	−0.42		
3742.280	2713.24	a ^{5}F$_2$	29 427.32	z ^{5}F°$_2$	3.53(8)	−0.13	3.16(8)	−0.18
3742.800	15 550.16	a ^{3}H$_6$	42 260.53	z ^{3}I°$_7$	1.27(9)	0.43		
3743.326	16 190.61	a ^{3}D$_3$	42 897.23	v ^{3}D°$_2$	1.02(8)	−0.66		
3745.594	12 207.05	a ^{3}G$_5$	38 897.50	z ^{3}H°$_6$	1.32(9)	0.44		
3753.537	12 816.69	a ^{3}G$_4$	39 450.66	y ^{3}G°$_5$	3.65(8)	−0.11		
3755.928	12 816.69	a ^{3}G$_4$	39 433.70	y ^{3}F°$_3$	4.55(8)	−0.02		
3759.837	7483.07	a ^{5}D$_4$	34 072.41	z ^{5}P°$_3$	1.71(8)	−0.44	1.42(8)	−0.52
3760.015	3105.49	a ^{5}F$_1$	29 693.57	z ^{5}F°$_1$	2.27(8)	−0.32	2.03(8)	−0.37
3761.507	13 699.07	a ^{3}G$_3$	40 276.61	y ^{3}G°$_4$	3.22(8)	−0.17		
3764.030	14 700.32	a ^{1}G$_4$	41 260.04	x ^{3}F°$_3$	2.00(8)	−0.37		
3767.350	13 699.07	a ^{3}G$_3$	40 235.39	y ^{3}G°$_3$	3.30(8)	−0.15		
3786.050	2713.24	a ^{5}F$_2$	29 118.49	z ^{5}D°$_1$	2.06(8)	−0.36	1.82(8)	−0.41
3790.515	2091.54	a ^{5}F$_3$	28 465.69	z ^{5}D°$_2$	3.49(8)	−0.13	3.05(8)	−0.18
3798.898	1190.64	a ^{5}F$_4$	27 506.59	z ^{5}D°$_3$	4.83(8)	0.02	4.19(8)	−0.04
3799.349	0.00	a ^{5}F$_5$	26 312.83	z ^{5}D°$_4$	5.17(8)	0.05	4.80(8)	0.02

Table 2 – *continued*

λ (Å)[a]	Lower level		Upper level		Theory		Experiment	
	E (cm^{-1})[b]	Desig.[b]	E (cm^{-1})[b]	Desig.[b]	gA (s^{-1})[c]	log gf[c]	gA (s^{-1})[d]	log gf[d]
3808.685	14 700.32	a ^{1}G$_4$	40 948.65	z ^{1}F$^\circ_3$	1.27(8)	−0.56		
3812.729	12 816.69	a ^{3}G$_4$	39 037.18	z ^{1}G$^\circ_4$	2.98(8)	−0.19		
3814.842	15 054.07	a ^{3}D$_2$	41 260.04	x ^{3}F$^\circ_3$	2.55(8)	−0.26		
3817.293	15 550.16	a ^{3}H$_6$	41 739.30	x ^{3}G$^\circ_5$	7.66(8)	0.22		
3822.087	16 190.61	a ^{3}D$_3$	42 346.90	x ^{3}F$^\circ_4$	5.73(8)	0.10		
3824.936	10 623.53	a ^{3}P$_2$	36 760.34	y ^{3}D$^\circ_3$	1.05(8)	−0.64	9.59(7)	−0.68
3831.793	12 207.05	a ^{3}G$_5$	38 297.09	z ^{3}H$^\circ_5$	3.31(8)	−0.14		
3839.698	12 207.05	a ^{3}G$_5$	38 243.38	y ^{3}F$^\circ_4$	3.97(8)	−0.06		
3840.987	15 550.16	a ^{3}H$_6$	41 577.75	z ^{3}I$^\circ_6$	1.12(8)	−0.61		
3852.125	17 045.97	a ^{1}D$_2$	42 998.31	y ^{1}F$^\circ_3$	1.56(8)	−0.46		
3857.541	14 700.32	a ^{1}G$_4$	40 616.22	z ^{1}H$^\circ_5$	8.81(8)	0.29		
3862.682	17 096.87	a ^{3}H$_4$	42 978.28	z ^{3}I$^\circ_5$	6.29(8)	0.15		
3891.426	16 190.61	a ^{3}D$_3$	41 880.85	v ^{3}D$^\circ_3$	3.84(8)	−0.06		
3909.082	13 699.07	a ^{3}G$_3$	39 273.28	z ^{3}H$^\circ_4$	3.72(8)	−0.07		
3923.474	12 816.69	a ^{3}G$_4$	38 297.09	z ^{3}H$^\circ_5$	5.58(8)	0.11		
3931.762	12 816.69	a ^{3}G$_4$	38 243.38	y ^{3}F$^\circ_4$	1.56(8)	−0.44		
3945.584	16 240.13	a ^{3}H$_5$	41 577.75	z ^{3}I$^\circ_6$	5.40(8)	0.10		
4051.391	8770.93	a ^{5}P$_3$	33 446.84	y ^{5}D$^\circ_4$	1.70(8)	−0.37	1.49(8)	−0.43
4068.365	14 700.32	a ^{1}G$_4$	39 273.28	z ^{3}H$^\circ_4$	1.97(8)	−0.31		
4080.594	6545.03	a ^{3}F$_4$	31 044.35	z ^{3}D$^\circ_3$	4.00(8)	0.00	3.68(8)	−0.04
4097.782	9183.66	a ^{3}F$_2$	33 580.22	z ^{3}D$^\circ_1$	1.24(8)	−0.51	1.08(8)	−0.57
4112.740	8084.12	a ^{3}F$_3$	32 391.95	z ^{3}F$^\circ_3$	1.60(8)	−0.39	1.65(8)	−0.38
4167.514	9183.66	a ^{3}F$_2$	33 172.02	z ^{3}F$^\circ_2$	1.10(8)	−0.55	9.45(7)	−0.61
4175.428	20 055.71	a ^{1}H$_5$	43 998.60	2°(^{5}G°)$_6$	1.08(8)	−0.54		
4199.894	6545.03	a ^{3}F$_4$	30 348.45	z ^{3}F$^\circ_4$	3.71(8)	−0.37	3.59(8)	−0.02
4206.015	8084.12	a ^{3}F$_3$	31 852.90	z ^{3}G$^\circ_3$	1.43(8)	−0.43	1.09(8)	−0.54
4212.063	6545.03	a ^{3}F$_4$	30 279.68	z ^{5}G$^\circ_5$	2.93(8)	−0.11	2.39(8)	−0.20
4214.439	13 645.75	b ^{3}P$_2$	37 367.02	x ^{5}D$^\circ_3$	1.97(8)	−0.28	1.87(8)	−0.30
4225.103	20 242.01	a ^{1}P$_1$	43 903.41	y ^{1}D$^\circ_2$	1.51(8)	−0.39		
4255.396	20 055.71	a ^{1}H$_5$	43 548.67	y ^{3}H$^\circ_6$	3.87(8)	0.02		
4258.988	13 645.75	b ^{3}P$_2$	37 118.90	z ^{3}P$^\circ_2$	1.06(8)	−0.54	6.80(7)	−0.73
4297.708	8084.12	a ^{3}F$_3$	31 345.79	z ^{5}G$^\circ_4$	3.37(8)	−0.03	2.98(8)	−0.08
4307.593	9183.66	a ^{3}F$_2$	32 391.95	z ^{3}F$^\circ_3$	1.29(8)	−0.45	8.89(7)	−0.61
4349.704	13 981.67	b ^{3}P$_1$	36 965.28	y ^{3}D$^\circ_2$	1.10(8)	−0.50	1.01(8)	−0.55
4390.439	8575.42	a ^{5}D$_3$	31 345.79	z ^{5}G$^\circ_4$	1.06(8)	−0.52	1.06(8)	−0.51
4410.025	9183.66	a ^{3}F$_2$	31 852.90	z ^{3}G$^\circ_3$	1.47(8)	−0.37	1.32(8)	−0.37
4460.026	8770.93	a ^{5}P$_3$	31 186.03	z ^{5}S$^\circ_2$	1.17(8)	−0.48	1.12(8)	−0.48
4554.517	6545.03	a ^{3}F$_4$	28 495.10	z ^{3}G$^\circ_5$	4.09(8)	0.11	3.80(8)	0.07
4584.443	8084.12	a ^{3}F$_3$	29 890.91	z ^{3}G$^\circ_4$	1.45(8)	−0.34	8.98(7)	−0.55
4645.099	20 055.71	a ^{1}H$_5$	41 577.75	z ^{3}I$^\circ_6$	2.67(8)	−0.06		
4709.481	9120.63	b ^{3}F$_4$	30 348.45	z ^{3}F$^\circ_4$	1.29(8)	−0.37	1.41(8)	−0.33

[a]Wavelengths (in air) are deduced from experimental levels compiled by Moore (1971).
[b]From Moore (1971).
[c]This work (HFR+CPOL approach).
[d]From Wickliffe et al. (1994).

even by spectral synthesis. We give the same weight to the six lines.

The lines of the major ionization stage, Ru II, are unfortunately too faint to be observed. This point could be easily verified by considering a new set of oscillator strengths obtained in this ion using methods similar to those described in this paper, i.e. TR-LIF measurements combined with HFR calculations (Palmeri et al. 2008).

The ruthenium abundance has been derived with two different models of the solar photospheric layers, the classical and often used 1D model of Holweger & Müller (1974) and a new 3D, time-dependent, hydrodynamical model recently developed by Trampedach et al. (in preparation). These 3D models are remarkably successful in reproducing the observed solar granulation topology, the observed shifts, widths and asymmetries of the lines profiles, none of which 1D models are able to predict. They also successfully reproduce the observed centre-to-limb variation of the continuum as a function of wavelength as well as the wings of the hydrogen Balmer lines (see e.g. Asplund et al. 2009; Pereira, Asplund & Trampedach, in preparation).

With the new oscillator strengths obtained in this work, the mean ruthenium abundance is 1.70 ± 0.11, whereas, with the experimental log gf values from Wickliffe et al. (1994), the mean ruthenium abundance becomes 1.74 ± 0.12. These abundances, which differ by only 10 per cent, are obtained with two different sets of accurate transition probabilities. We will recommend the mean value of these results, 1.72 ± 0.10, as the photospheric abundance of ruthenium. Taking the mean of the two gf scales on a line-by-line basis and

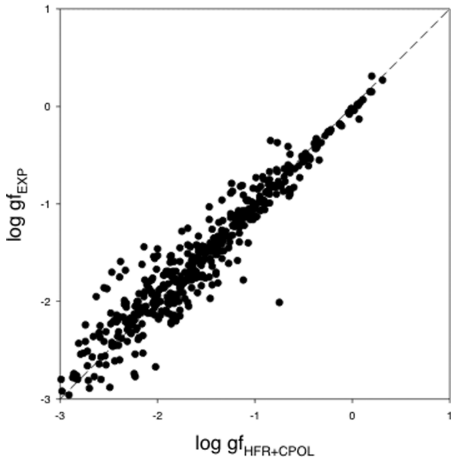

Figure 1. Comparison between calculated oscillator strengths (log *gf*) as obtained in this work (HFR+CPOL) and experimental values (EXP) published by Wickliffe et al. (1994).

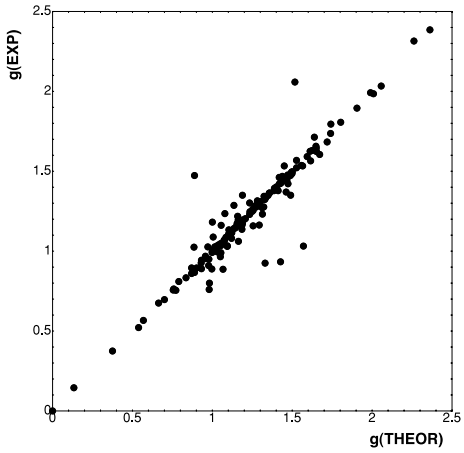

Figure 2. Comparison between calculated (THEOR) and experimental (EXP) Landé *g* factors.

then taking the standard deviation in fact results in 1.72 ± 0.10. This result is in agreement with the most recent meteoritic abundance of ruthenium, 1.76 ± 0.03, by Lodders, Palme & Gail (2009). The rather large dispersion of the results is due to the uncertainties in the equivalent widths measurements. As already mentioned, these lines are very difficult to measure accurately. We checked that spectral synthesis could not improve upon the accuracy of the derived ruthenium abundances.

We note that the abundance obtained with the 1D model of Holweger & Müller (1974), traditionally used in solar abundance analyses, is 0.20 dex larger i.e. $A_{\rm Ru} = 1.92$ and thus inconsistent with the meteoritic abundance. Such a large difference is expected for the highly temperature-sensitive Ru I lines.

7 LANDÉ *G* FACTORS

Investigating the magnetic properties of the atoms is fundamental in many fields of physics. In particular, a detailed knowledge of the Landé *g* factors is important to analyse the atomic spectra when an external magnetic field is applied. It can also provide a useful information regarding the spin-orbit interaction and, consequently, the coupling schemes met in the atoms. Moreover, the *g* factor is helpful for the assignment of the energy levels in terms of analysis and allows us to get a deeper insight into the properties of Rydberg states of atoms. In astrophysics, a severe limitation to stellar magnetic field determinations is frequently related to the lack of accurate Landé *g* factors.

In Ru I, many experimental *g* values are reported in Moore's (1971) compilation. They are compared in Fig. 2 with the theoretical results calculated in this work. The agreement is within 5 per cent for most of the levels. Larger discrepancies (>20 per cent) are observed for the five levels at 32 207.65, 32 343.30, 43 975.79, 44 243.49 and 44 662.01 $\rm cm^{-1}$. As these discrepancies do not seem to be due to erroneous assignments of the levels, they could perhaps be explained by possible errors affecting the 'old' measurements (Meggers & Laporte 1926; Sommer 1926; Harrison & McNally 1940; McNally 1941). Their origin, however, is unclear and new measurements would be welcome to definitely settle this question.

For a number of levels, there are no experimental *g* values available (if we except the tentative value for 23 004.77 $\rm cm^{-1}$) and, consequently, we report in Table 4 the corresponding HFR+CPOL results.

8 CONCLUSIONS

A new set of transition probabilities has been obtained for many transitions in Ru I of astrophysical interest using a HFR+CPOL

Table 3. Ru I transitions of solar interest. We report successively the wavelengths (λ), the lower excitation energies ($E^b{}_{\rm low}$), the equivalent widths (W_λ), the oscillator strengths (log *gf*) and the abundance values ($A_{\rm Ru}$) as deduced in this work in the usual logarithmic scale.

λ (Å)[a]	$E^b{}_{\rm low}$ (eV)	$W^c{}_\lambda$ (mÅ)	log gf[d] Theoretical	$A^e{}_{\rm Ru}$ 3D	$A^e{}_{\rm Ru}$ 1D	log gf[f] Experimental	$A^e{}_{\rm Ru}$ 3D	$A^e{}_{\rm Ru}$ 1D
3436.736	0.148	10.0 ± 2.0	0.18	1.54	1.75	0.15	1.57	1.78
3498.942	0.000	20.5 ± 2.0	0.20	1.80	1.98	0.31	1.69	1.87
3742.280	0.336	7.4 ± 0.4	−0.13	1.80	2.00	−0.18	1.85	2.05
4080.594	0.812	2.8 ± 0.3	0.00	1.63	1.82	−0.04	1.67	1.86
4554.517	0.812	5.5 ± 0.7	0.11	1.77	1.97	0.07	1.81	2.01
4584.443	1.002	1.05 ± 0.2	−0.34	1.66	1.85	−0.55	1.87	2.06

[a]Wavelengths (in air) deduced from experimental levels compiled by Moore (1971).
[b]From Moore (1971).
[c]This work: measured on the solar spectrum of Delbouille et al. (1973) and of Neckel & Labs (1984).
[d]This work: HFR + CPOL approach (see the text).
[e]3D: model of Trampedach et al. (in preparation), 1D: model of Holweger & Müller (1974).
[f]From Wickliffe et al. (1994).

Table 4. HFR+CPOL Landé g factors for Ru I levels for which no experimental results are available.

Level (cm^{-1})	Desig.[a]	g value	Level (cm^{-1})	Desig.[a]	g value
23 004.77	$4d^6 5s^2$ b $^3H_4$	0.977	29 890.91	$4d^7 5p$ z $^3G^\circ_4$	1.173
24 927.48	$4d^6 5s^2$ d ^3P?	1.463	29 891.90	$4d^6 5s5p$ z $^7F^\circ_3$	1.497
25 602.60	$4d^6 5s^2$ b $^3G_5$	1.179	29 979.00	$4d^6 5s^2$ b $^3D_3$	1.330
25 642.69	$4d^6 5s^2$ b $^3G_4$	1.091	30 085.38	$4d^6 5s5p$ z $^7F^\circ_1$	1.502
26 075.70	$4d^6 5s^2$ b $^3G_3$	0.898	42 404.14?	$4d^7 5p$ z $^1I^\circ_6$	1.160
26 780.46	$4d^6 5s5p$ z $^7D^\circ_1$	2.986	42 897.23	v $^3D^\circ_2$	1.414
27 289.24	$4d^7 5s$ d $^3F_4$	1.174	42 939.12	$4d^7 5p$ x $^3G^\circ_4$	1.488
27 560.59	$4d^6 5s^2$ d $^3P_1$?	1.383	43 862.91	w $^3G^\circ_4$	1.071
27 516.57	$4d^7 5s$ d $^3F_3$	0.977	44 607.61	$4d^6 5s5p$ x $^5F^\circ_4$	0.856
29 352.41	$4d^6 5s^2$ b $^3D_2$	1.177	44 800.81	$4d^6 5s5p$ x $^5F^\circ_3$	0.667

[a]From Moore (1971). The question marks are taken from this compilation.
Only the levels with energies $<45\,000\,cm^{-1}$ have been considered (see the text).

atomic model firmly assessed through comparisons of theoretical lifetimes with TR-LIF measurements previously available or new measurements performed in this work at the Lund Laser Center (Sweden). The comparisons between theoretical and experimental f values, shown in Table 2, indicate that the new results are accurate (within 10–15 per cent), particularly for the strongest transitions. These new results will help astrophysicists in their stellar analyses. The solar abundance of ruthenium has been revised and the new photospheric value is in close agreement with the meteoritic value found in carbonaceous chondrites.

ACKNOWLEDGMENTS

This work was financially supported by the Integrated Initiative of Infrastructure Project LASERLAB-EUROPE, contract 212 025, the Swedish Research Council through the Linnaeus grant and the Belgian FRS-FNRS. EB, PQ and PP are, respectively, Research Director, Senior Research Associate and Research Associate of the FRS-FNRS. VF acknowledges a fellowship from FRIA.

REFERENCES

Allen D. M., Porto de Mello G. F., 2008, A&A, 474, 221
Asplund M., 2005, ARA&A, 43, 481
Asplund M., Grevesse N., Sauval A. J., Scott P., 2009, ARA&A, in press
Biémont É., 2005, Phys. Scr., T119, 55
Biémont É., Quinet P., 2003, Phys. Scr., T105, 38
Biémont É., Grevesse N., Kwiatkovski M., Zimmermann P., 1984, A&A, 131, 364
Corliss C. H., Bozman W. R., 1962, Experimental Transition Probabilities for Spectral Lines of Seventy Elements. Natl. Bur. Stand., US, Monogr. 53
Cowan R. D., 1981, The Theory of Atomic Structure and Spectra. University of California Press, Berkeley, CA
Delbouille L., Neven L., Roland G., 1973, Atlas Photométrique du Spectre Solaire de 3000 á 10000 Å. Institut d'Astrophysique, Université de Liège, Liège
Fivet V., Palmeri P., Quinet P., Biémont É., Xu H. L., Svanberg S., 2006, Eur. Phys. J. D, 37, 29
Fraga S., Karwowski J., Saxena K. M. S., 1976, Handbook of Atomic Data. Elsevier, Amsterdam
Harrison G. R., McNally J. R., Jr., 1940, Phys. Rev., 58, 703
Holweger H., Müller E. A., 1974, Sol. Phys., 39, 19
Jaschek M., Brandi E., 1972, A&A, 20, 233
Kessler K. G., Meggers W. F., 1955, J. Res. Nat. Bur. Stand., 55, 97
Krishnaswamy K., Sneden C., 1985, PASP, 97, 407
Lodders K., Palme H., Gail H. P., 2009, Landoldt-Börnstein series in Astronomy and Astrophysics, in press
McNally J. R., Jr., 1941, Thesis, MIT, Cambridge, MA
Meggers W. F., Laporte O., 1926, J. Wash. Acad. Sci., 16, 143
Moore C. E., 1971, Atomic Energy Levels, NSRDS-NBS 35
Neckel H., Labs D., 1984, Sol. Phys., 90, 205
Nilsson H., Engström L., Lundberg H., Palmeri P., Fivet V., Quinet P., Biémont É., 2008, Eur. Phys. J. D, 49, 13
Orlov M. Ya., Shavrina A. V., 1990, Astrophys., 32, 126
Palmeri P., Quinet P., Fivet V., Biémont É., Nilsson H., Engström L., Lundberg H., 2008, Phys. Scr., 015304
Quinet P., Palmeri P., Biémont É., McCurdy M. M., Rieger G., Pinnington E. H., Wickliffe M. E., Lawler J. E., 1999, MNRAS, 307, 934
Salih S., Lawler J. E., 1985, J. Opt. Soc. Am. B, 2, 422
Smith V. V., Wallerstein G., 1983, ApJ, 273, 742
Sommer L. A., 1926, Z. Phys., 37, 1
Thévenin F., 1989, A&AS, 77, 137
Thévenin F., 1990, A&AS, 82, 179
Wickliffe M. E., Salih S., Lawler J. E., 1994, J. Quant. Spectrosc. Radiat. Transfer., 51, 545
Xu H. L., Svanberg S., Quinet P., Garnir H. P., Biémont É., 2003, J. Phys. B: At. Mol. Opt. Phys., 36, 4773
Xu H. L. et al., 2004, Phys. Rev. A, 70, 042508

This paper has been typeset from a TEX/LATEX file prepared by the author.